A Chainring-Integrated Pedal-Assisted Electric Bicycle System

by

Jinyu Chen

Researched in the field of Physics and Computer Science
in partial fulfillment of the requirements for the

Interdisciplinary Research Project

at the

BEIJING NATIONAL DAY SCHOOL

June 2025

Author_____

Jinyu Chen
Physics and Computer Science
June 23, 2025

Advisor_____

Jiangfan Han

A Chainring-Integrated Pedal-Assisted Electric Bicycle System

by

Jinyu Chen

Abstract

This paper presents the design, manufacturing, and experiment of a chainring-integrated pedal-assisted electric bike system that enhances accessibility, efficiency, and modularity. Addressing the limitations of current e-bike designs, the system integrates a BLDC motor into the chainring and uses field-oriented control (FOC) for responsive and natural torque assistance. Key innovations include a compact direct-drive structural architecture and torque-based assist algorithms. The prototype was built with 3D-printed components, demonstrating effective performance in lab tests. While refinement on system robustness is needed, the system offers a novel, cost-effective solution for general riders.

Contents

Chapter 1

Introduction

Today, as the global population ages, problems such as declining motor ability, respiratory function, and physical performance become increasingly prevalent. These challenges are exacerbated by the highly sedentary modern lifestyle and the lack of accessible, low-intensity physical activity suitable for elderly individuals. Cycling is positioned to be suitable for this scenario due to its low requirement for junction functionality and demand for rapid, multidimensional muscle coordination and movement. Consequently, improving the accessibility of cycling may mitigate this problem by promoting participation for the aged population in a low-injury risk sport.

To this end, we designed and developed the chainring-integrated pedal-assisted electric bike system specifically for this population. Specifically, a paddle-assisted electric biking system refers to the principle wherein motor assistance is only activated in response to active rider input, thereby augmenting human effort instead of obsoleting it. We introduce a novel mechanism for a pedal-assist e-bike that is low-cost, upgradable, and capable of more direct torque transmission.

1.1 Overview of Existing Solutions

1.1.1 Mid-Drive Motor

Currently, mid-drive motors are the most advanced implementation of e-bike systems, featuring high power, custom frame integration, and a battery pack embedded within the bike's down tube, as shown in Figure 1-1. However, this type of system often requires a proprietary frame that is specifically designed for e-bikes and is not upgradable from regular bicycles. This system often comes with a stock bike only, making it very expensive for the general public. Furthermore, replacing the integrated battery is difficult once it deteriorates.

Figure 1-1: Example of a mid-drive motor. The motor and gearbox are located on the bottom bracket of a proprietary bike frame.

1.1.2 Hub Motor

Hub motor solution is a motor installed within the front or rear wheel hubs, as shown in Figure 1-2. It is a feasible approach featuring a lower price, the ability to be upgraded from a regular bike, and highly customizable specifications for high compatibility. The shortcoming of the solution is that the torque is applied at the wheel rather than at the crank, and it is difficult to dynamically detect rider input

and adjust motor output accordingly. This results in an unnatural and less intuitive riding experience for riders.

Figure 1-2: Example of a hub motor. A hoverboard motor is attached to the hub of the wheel with customized spokes connecting the rim.

1.1.3 Friction Drive Solution

Friction drive systems use external motors that drive the wheel via friction, as shown in Figure 1-3. Although it is simple and cheap, this solution is nearly obsolete due to its poor transmission efficiency, bulky appearance, and underwhelming performance.

Figure 1-3: Example of a friction-driven motor. The power is transmitted through friction between the small wheel and the bicycle rear wheel.

1.2 Advantage of a Chainring Integrated System

In this paper, a new solution addressing the aforementioned problems of upgrade ability, price, riding experience, and system complexity is proposed and developed. This solution integrates a brushless direct current motor (BLDC), controlled by field-oriented control (FOC), directly to the bottom bracket. A customized chainring is then attached to the motor without any gear reduction mechanisms, featuring high power transmission efficiency, direct drive, and enhanced performance.

Chapter 2

Design

2.1 Mechanical Design

The design of the chainring-integrated e-bike system is built to meet the goal of being low-cost in manufacturing, upgradable and dismountable, and natural in power transmission. The system consists of an adapter that is fixed on the bottom bracket of the frameset of the bike, a chainring integrated with a BLDC motor that connects to the adapter, a crankset, an FOC control module, and a battery pack. As shown in Figure 2-1, the motor integrated in the chainring is the torque source of the assisting system, and can be controlled to output precise torque, velocity, and position. The hollow magnetic encoder is housed on the same side of the motor around the central axle to ensure the precision and accuracy of the position data, which is indispensable for FOC control. The central axle is connected to the motor rotor and chainring, as shown in Figure 2-2. The crank on the drive side is unibody with the chainring, while the non-drive side crank is connected with the axle through a spline. The chainring-crankarm set is shown in Figure 2-3.

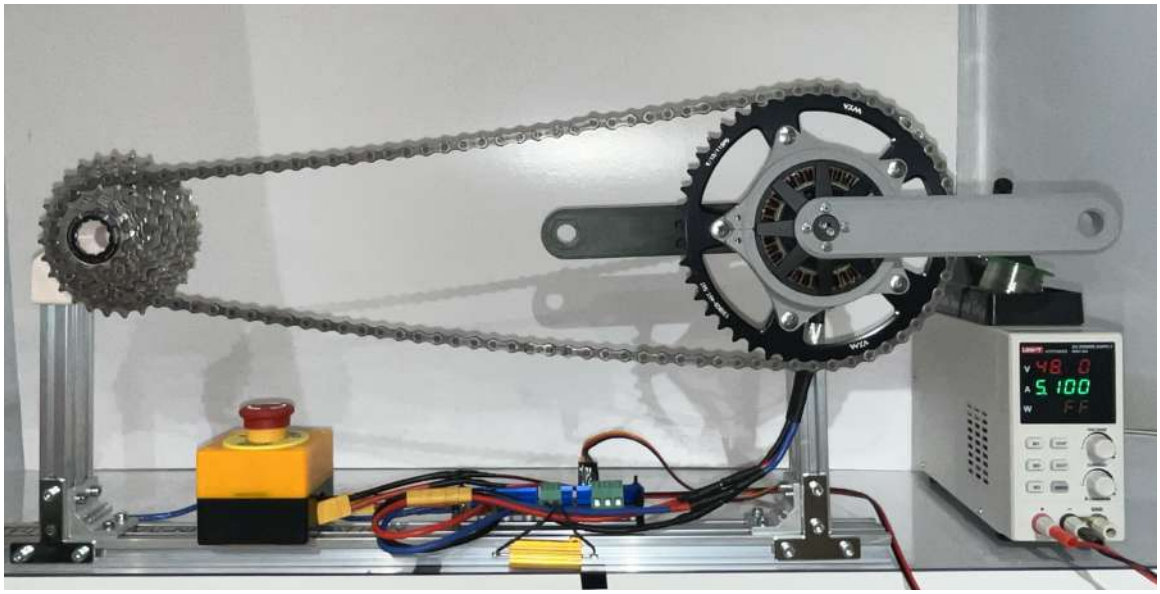

Figure 2-1: Overview of the system on the lab test stand.

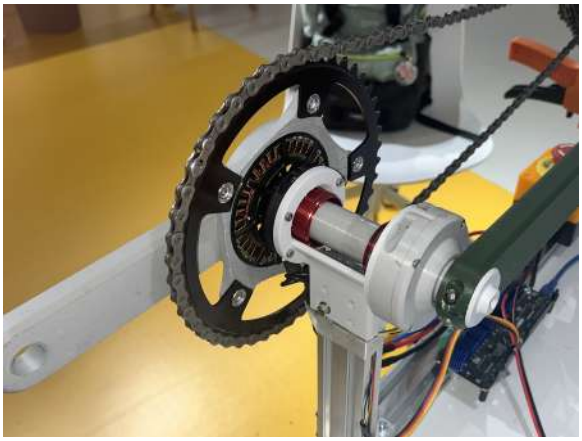

Figure 2-2: The chainring from behind. The axle is attached to the motor rotor, and the encoder is on the non-drive side.

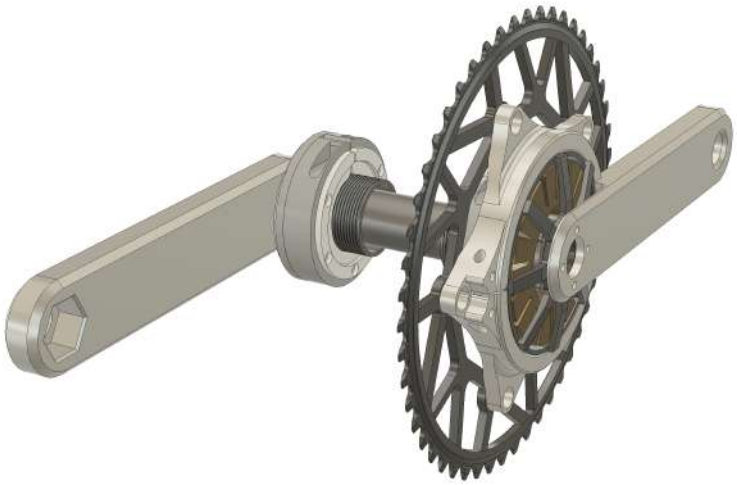

Figure 2-3: Fully integrated chainring-crankarm set

2.1.1 Motor

The motor used in this project is CrazyMotor 8108 100KV outrunner BLDC with a rotor diameter of 81mm, a thickness of 8 mm, 40 magnetic poles and 36 teeth, and a velocity constant of 100 revolutions per minute per volt applied to the motor, as shown in Figure 2-4 and 2-5. The motor is deliberately chosen to meet the requirements of this application: the motor must be capable of generating high torque up to 10Nm under low angular velocity down to 90 revolutions per minute. Therefore, a disc-shaped outrunner BLDC motor would best suit this use as it features a higher rotor inertia and a plethora of internal space for an increased number of turns of winding, since more winding turns can increase the magnetic field strength, leading to a higher torque performance.

Figure 2-4: CAD model of a 8108 BLDC Motor

Figure 2-5: Motor integrated into the chainring. The copper wire is wound on the stator of the motor.

2.1.2 Integrated Chainring

The chainring in the system acts as a bridge between human and motor power as it connects to both the pedal and the motor. Unlike most commercially prevailing products, where the chainring, spider(the component connecting the chainring and right-side crank), and crank are separate and assembled by bolts, this system, as shown in Figure 2-6, Figure 2-7, and Figure 2-8, integrates the motor, spider, and crank into a unibody crankset, where a regular 5-hole 130BCD chainring can be installed using standard bolts, ensuring its compatibility with standarized bike components that is consumable after repeated use.

Figure 2-6: Integrated chainring, spider, crankarm, and motor

Figure 2-7: Integrated chainring, spider, crankarm, and motor from behind

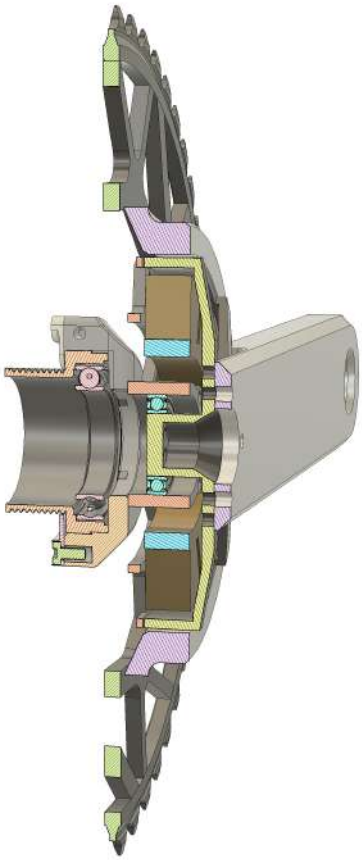

Figure 2-8: Integrated chainring, spider, crankarm, and motor section view

2.1.3 Motor Mount

The motor mount is the connector between the bike frameset and the motor stator. It is essential since it is where the torque is applied against the frame and propels the chainring. In this system, the motor mount is connected to a standard threaded bottom bracket(in a regular bicycle, the bottom bracket houses bearing on each sides and is screwed-in or pressed-in to the bottom bracket shell, where the crankset axle penetrates) using a dual-layer structure, as shown in Figure 2-9, Figure 2-10, and Figure 2-11. The first layer connects with the stator of the motor and secures a BB53

regular bottom bracket using splines, ensuring rigid torque transmission; the second layer is a lock ring attached to the first layer from behind, further constraining the bottom bracket. Finally, the bottom bracket, covered with the sandwiched structure, can be screwed into the bottom bracket shell, connecting the motor and frameset, provided that the frameset complies with the BSA specification, which is now widely used for commercial bikes.

Figure 2-9: The motor mount connecting the frameset and the motor stator covers a standard bicycle bottom bracket

Figure 2-10: The motor mount connecting the frameset and the motor stator covers a standard bicycle bottom bracket from behind

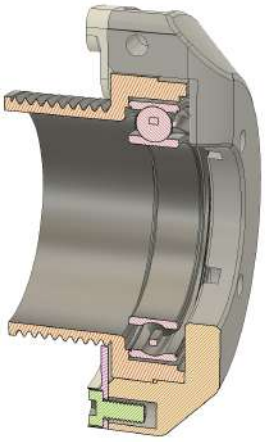

Figure 2-11: The motor mount connecting the frameset and the motor stator covers a standard bicycle section view

2.1.4 Encoder Housing

In field-oriented control, precise and instant position sensing is critical. Consequently, the encoder must be installed where the deviation from the motor's actual position is within the tolerance of the control system. Given the intrinsic structure of the bicycle crankset, on-axis encoders cannot be fixed relative to the frame on one end of the motor shaft. Therefore, a hollow, off-axis encoder is used to avoid conflict with the motion of the crank. The encoder PCB is housed on the non-drive side, connected with the bottom bracket, as shown in Figure 2-12, Figure 2-13, and Figure 2-14. The magnetic ring that carries the position index is secured on the axle, as shown in Figure 2-15. This structure ensures that the encoder is close enough to the motor to collect less noisy data.

Figure 2-12: The encoder mount connecting the frameset and the encoder covers a standard bicycle bottom bracket

Figure 2-13: The encoder mount connecting the frameset and the encoder covers a standard bicycle bottom bracket from behind

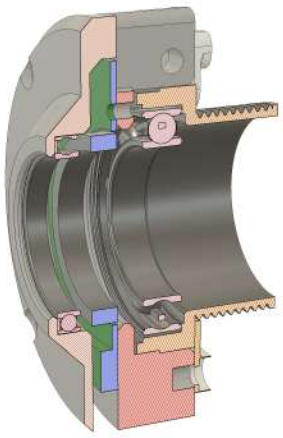

Figure 2-14: The encoder mount connecting the frameset and the encoder covers a standard bicycle bottom bracket section view

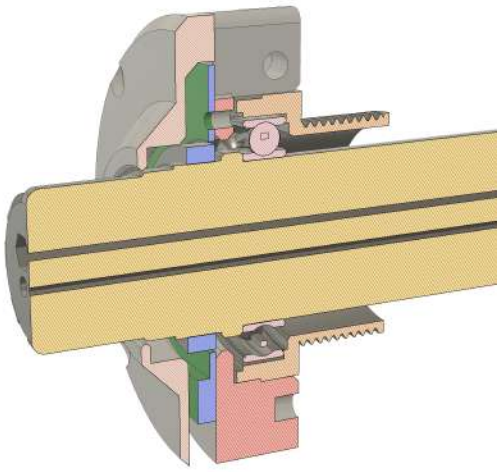

Figure 2-15: Section view of the encoder mount and the axle. The green PCB detects the position of the purple-section magnetic ring.

2.2 Control

The direct mounting of the motor on the chainring, while enhancing efficiency, accessibility, and user experience, poses a challenge to the control of the motor, as any misalignment or cogging can be sensed by the user and potentially ruin the user experience and pose safety issues. To this end, a robust closed-loop control scheme over torque, velocity, and position is employed as opposed to the open-loop control scheme, where there is no feedback on motor actuation for it to self-correct control failures and abnormalities. Odrive Overview This project uses the ODrive 3.6 56V motherboard, an open-source FOC controller supporting closed-loop torque, velocity, and position control, as shown in Figure 2-16 and Figure 2-17. ODrive offers affordable, real-time control with highly customizable PID loop parameters. Communication with the control terminal is achieved via a serial interface.

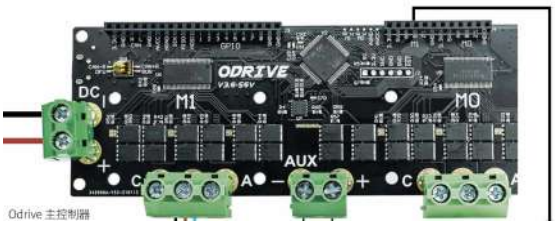

Figure 2-16: The ODrive 3.6 56V motherboard

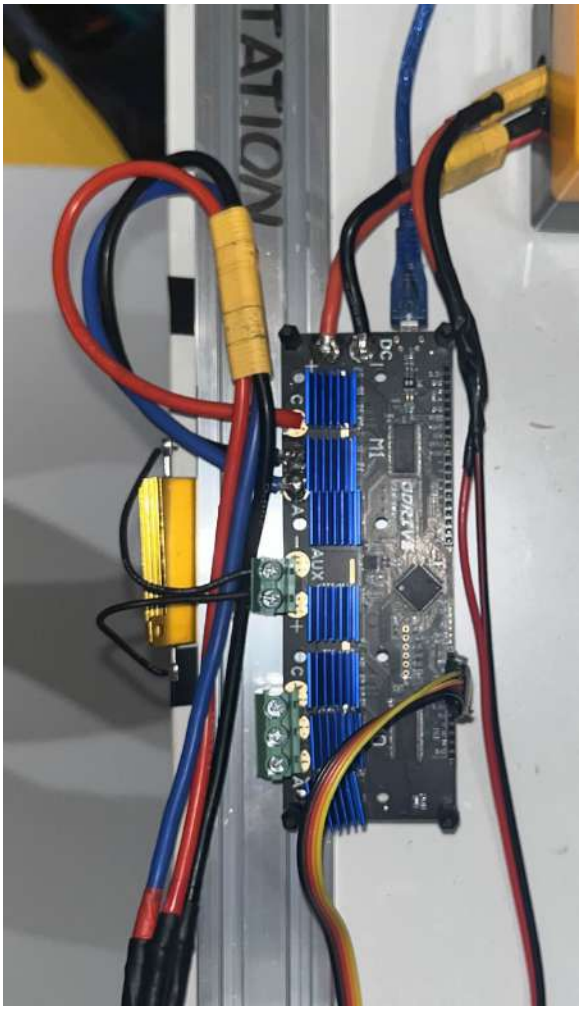

Figure 2-17: Odrive in the lab, connected to the motor and the encoder.

2.2.1 Encoder

The encoder used in this system is an MGT-INC_3154F off-axis magnetic incremental encoder, featuring up to 14-bit resolution and 1024 ppr, as shown in Figure 2-18 and Figure 2-19. The encoder communicates via an ABZ non-differential signal with an index. This setup ensures an acceptable level of noise in the electromagnetic field environment and provides high-fidelity position feedback.

Figure 2-18: CAD model of the encoder

Figure 2-19: Encoder mounted on the test stand

2.2.2 Current and Torque Control

As the ultimate goal of this project is to provide riders with smoother motor assistance, the main focus of the motor control is on torque. This is because the goal of velocity and position control is to achieve a certain stable state, whether a constant angular speed or a fixed position. On the contrary, torque control is dynamic. Torque control is the most intuitive mode of assistance because human effort manifests first as torque, not speed or position. Therefore, a smooth assistive algorithm should monitor the human riders' torque input and dynamically adjust motor torque. In Odrive, torque control is achieved by running a PI loop on quadrature-axis current, or Iq, derived from vectorized three-phase current via the Clarke and Park transforms. Iq is directly proportional to the torque, which is computed as

$$\tau = k_t \cdot I_q \quad \text{(in Nm)}$$

Where k_t is the torque constant, determined by

$$k_t = \frac{8.27}{K_v} \quad \text{(in Nm/A)}$$

2.3 Power Assist Algorithm

2.3.1 Velocity-Based Torque Amplification

This algorithm is a passive assisting mode that supplements riders' effort by magnifying their torque. Position data from the encoder is used to calculate the instantaneous angular velocity and angular acceleration. Rider torque is estimated based on the angular acceleration and calculated system inertia, factoring in the motor, crankset, and rider leg mass. The assistive torque will be applied by the motor proportional to the

rider's torque, amplifying the rider's power output. The amplification will increase at a decreasing rate as the rider torque increases to prevent overspeed. The intensity of the assistance is adjustable through gain coefficients. This mode is suitable for highly intermittent power output scenarios, such as consecutively undulating routes, featuring dynamic assistance.

2.3.2 Torque Compensation

In this mode, a target torque is specified, and the motor will compensate for any torque gap between the rider's torque output and the target. Every target torque corresponds to a certain terminal speed of the bike because the air resistance scales with speed, and the bike will travel at a constant speed when the traction force and the air resistance cancel out. In lab testing, air resistance is modeled and integrated into the torque control loop to emulate real-world conditions. As a result, this mode is suitable for cruising at a specific speed on uniform gradients.

Chapter 3

Manufacturing

3.1 Method

In the early development stage, the main focus of manufacturing is on proof of concept. Therefore, as opposed to metal manufacturing, such as Computer Numerical Control(CNC) milling or drilling, Fused Filament Fabrication(FFF) or Fused Deposition Modeling(FDM) 3D printing technology, known for its low-cost, rapid prototyping, and material versatility, is used for manufacturing most of the functional parts in this project.

For the housing of the motor, encoder, and battery pack, the material of polylactic acid, or PLA, is used for its ease of printing, low cost, and lightweight. However, PLA lacks the properties of strength and is susceptible to ultraviolet(UV), which makes it brittle and fragile under prolonged exposure. Therefore, functional parts such as the crankarm, axle, and chainring adapter are printed using a mixture of polycarbonate(PC) and acrylonitrile butadiene styrene(ABS) for durability and strength, even for prototyping.

All the parts are 3D modelled using Autodesk Fusion computer-aided design(CAD) software program and exported as a STEP file. Then, the 3D models will undergo slicing, where the model will be sliced into thin layers for printing to generate G-code, a programming language used to control automated machine tools, reflecting the movement of the printer's nozzle. Finally, the parts are printed using the Bambu Lab P1S 3D printer.

3.2 Post-Processing

Due to 3D printing's lack of precision and material stiffness, fasteners cannot be directly inserted and tightened. Therefore, for parts that needed to be assembled using fasteners, heat-staking insert brass nuts are used to create internal threads.

Chapter 4

Results

4.1 Effect of Algorithms

In a laboratory environment, both algorithms performed as intended. The system successfully amplified or compensated torque as designed.

4.2 Instability Analysis

From the results, spikes and instabilities in the detected torque and applied torque are present. These spikes and jumps in input data interfere with the algorithm, resulting in cogging and twitching. Analyzing the source of the errors, it can be attributed to the lack of structural stiffness and encoder misalignment due to inaccuracies of the 3D printed parts. They highlight the need for improved mechanical precision and more robust signal filtering algorithms in future iterations.

Chapter 5

Conclusions

5.1 Project Summary

In this project, a new approach to electric-assisted biking is proposed to solve the problem of cost, accessibility, and rider experience that current solutions suffer from. The design and manufacturing of this chainring-integrated pedal-assisted electric bike system, consisting of the motor, chainring-crankarm set, bottom bracket connector, and control system and algorithm, is documented in this paper. The prototype demonstrates successful operation under laboratory conditions, and the results validate the system's potential to address current e-bike limitations by offering a dismountable, direct-drive, and cost-friendly design, aimed at helping more physically limited individuals to enjoy the sport of cycling.

Bibliography

[1] A. Hattori, *Design of a high torque density modular actuator for dynamic robots*. PhD thesis, Massachusetts Institute of Technology, 2020.

[2] B. G. Katz, *A low cost modular actuator for dynamic robots*. PhD thesis, Massachusetts Institute of Technology, 2018.

[3] P. M. Wensing, A. Wang, S. Seok, D. Otten, J. Lang, and S. Kim, "Proprioceptive actuator design in the mit cheetah: Impact mitigation and high-bandwidth physical interaction for dynamic legged robots," *Ieee transactions on robotics*, vol. 33, no. 3, pp. 509–522, 2017.

[4] S. K. Challa, *Comparative study of axial flux permanent magnet brushless DC motor operating with the winding connected in single-phase and two-phase system*. Louisiana State University and Agricultural & Mechanical College, 2006.

[5] J. F. Gieras, R.-J. Wang, and M. J. Kamper, *Axial flux permanent magnet brushless machines*. Springer Science & Business Media, 2008.